0013-7227/00/$03.00/0
Endocrinology

Vol. 141, No. 4
Printed in U.S.A.

Vitamin D Is an Important Factor in Estrogen Biosynthesis of Both Female and Male Gonads*

KEIKO KINUTA, HIROYUKI TANAKA, TADASHI MORIWAKE, KUNIHIKO AYA, SHIGEAKI KATO, AND YOSHIKI SEINO

Department of Pediatrics, Okayama University Medical School (K.K., H.T., T.M., K.A., Y.S.), Okayama 700-8558; and Institute of Molecular and Cellular Biosciences (S.K.), University of Tokyo, Tokyo 113-0032, Japan

ABSTRACT

In the present study, the role of vitamin D in the regulation of estrogen synthesis in gonads was investigated. Vitamin D receptor null mutant mice showed gonadal insufficiencies. Uterine hypoplasia and impaired folliculogenesis were observed in the female, and decreased sperm count and decreased motility with histological abnormality of the testis were observed in the male. The aromatase activities in these mice were low in the ovary, testis, and epididymis at 24%, 58%, and 35% of the wild-type values, respectively. The gene expression of aromatase was also reduced in these organs. Elevated serum levels of LH and FSH revealed hypergonadotropic hypogonadism in these mice. The gene expressions of estrogen receptor α and β were normal in gonads in these mice. Supplementation of estradiol normalized histological abnormality in the male gonads as well as in the female. Calcium supplementation increased aromatase activity and partially corrected the hypogonadism. When the serum calcium concentration was kept in the normal range by supplementation, the aromatase activity in the ovary increased to 60% of the wild-type level, but LH and FSH levels were still elevated. These results indicated that vitamin D is essential for full gonadal function in both sexes. The action of vitamin D on estrogen biosynthesis was partially explained by maintaining calcium homeostasis; however, direct regulation of the expression of the aromatase gene should not be neglected. (*Endocrinology* **141:** 1317–1324, 2000)

1,25-DIHYDROXYVITAMIN D_3 [1,25-$(OH)_2D_3$], an active form of vitamin D, plays important roles in calcium homeostasis, bone metabolism, and cell differentiation and proliferation (1–3). Most of these actions are mediated by the nuclear vitamin D receptor (VDR) (4, 5). The VDR is expressed in calcium-regulating tissues such as intestine, skeleton, and parathyroid gland as well as in ovary and testis (6); however, VDR function in gonads remains unclear. VDR null mutant mice were established as a model for VDR itself and vitamin D function (7). In addition to the hypocalcemic rickets, uterine hypoplasia and impaired folliculogenesis were found in most of the female VDR null mutant mice, and estrogen supplementation increased the uterine weight of the mice (7). These results indicated that the uteri of the mice were in an estrogen-deficient state and suggested that VDR plays a role in estrogen production in the ovary. In male gonads, certain abnormalities may exist, although macroscopically the testis of the VDR null mutant male mice appeared normal.

To clarify the pathophysiology of the disorder of gonads in the VDR null mutant mice, the activity of aromatase cytochrome P450 (P450arom), a key enzyme in estrogen biosynthesis, and the expression of the CYP19 gene encoding P450arom (8) were investigated.

Received June 29, 1999.

Address all correspondence and requests for reprints to: Dr. Hiroyuki Tanaka, Department of Pediatrics, Okayama University Medical School, 2–5-1 Shikata-cho, Okayama 700-8558, Japan. E-mail: hrtanaka@hospital.okayama-u.ac.jp.

* This work was supported in part by a grant-in-aid for Scientific Research from the Ministry of Education, Science, Sports, and Culture of Japan and a grant from the Ministry of the Health and Welfare of Japan.

Materials and Methods

Materials

[1β-^{3}H]Androstenedione (24.7 Ci/mmol; catalogue no. NET926) was a product of NEN Life Science Products (Boston, MA). Glucose-6-phosphate, $NADP^+$, NADPH, glucose-6-phosphate dehydrogenase (230 U/mg solid), and 17β-estradiol were obtained from Sigma (St. Louis, MO). Dextran-coated charcoal was obtained from Yamasa (Choshi, Japan). *Taq* polymerase, 10 × PCR buffer, and 25 mM $MgCl_2$ were obtained from Perkin-Elmer Corp. (Branchburg, NJ). QIAamp tissue kit for the extraction of genomic DNA was purchased from QIAGEN (Hilden, Germany). A RT-PCR kit containing random primer, Moloney murine leukemia virus-reverse transcriptase, and 10 × first strand buffer was obtained from Stratagene (La Jolla, CA). A PCR MIMIC Construction Kit for competitive PCR was obtained from CLONTECH Laboratories, Inc. (Palo Alto, CA).

Animals

VDR null mutant mice were generated by gene targeting as described previously (7); the locus targeted for the disruption of the VDR gene included exon 2, and the mutant locus contained the neomycin resistance gene. Mice were weaned at 3 weeks of age and were then fed *ad libitum* distilled water and a chow diet (MF, Oriental Yeast, Tokyo, Japan; ingredients: 11.1 mg/g calcium, 8.3 mg/g phosphorus, and 1.08 IU/g vitamin D_3) or a high calcium diet (9) (Clea Japan, Inc., Tokyo, Japan; ingredients: 20.0 mg/g calcium, 12.5 mg/g phosphorus, 1.08 IU/g vitamin D_3, and 200 mg/g lactose). The mice were maintained under specific pathogen-free conditions with a 12-h light, 12-h dark cycle. They were bred as heterozygotes. The studies were reviewed and approved by the institutional committee of animal care and use of Okayama University Medical School.

The VDR genotypes were determined by analyzing genomic DNA obtained from each mouse at approximately 10 days after birth. Genomic DNA was extracted from tail clippings with the QIAamp tissue kit and was amplified by multiplex PCR using two sets of primers specific for the wild-type exon 2 of VDR gene and for the neomycin resistance gene, respectively. To this end, we recloned murine exon 2 of VDR gene and sequenced it. Novel primers with the sequences of 5′-CCT CCA TCC CTG TAA GAA GA-3′ and 5′-CAA AGA ACT GCC ACC CAC TC-3′

were prepared. Another set of primers (5′-TGA ATG AAC TGC AGG ACG AGG-3′ and 5′-AAG GTG AGA TGA CAG GAG ATC-3′) for detection of the neomycin resistance gene (10) was also prepared. The reaction mixture (50 μl) contained DNA template (4 μl), two of the primer sets (0.4 μM each), *Taq* polymerase (1 U), 5 μl of 10 × PCR buffer, $MgCl_2$ (1.5 mM), and a deoxy-NTP mixture (0.2 mM). The amplification included an initial denaturation step at 94 C for 5 min, followed by 30 cycles of denaturation at 94 C (1 min), annealing at 55 C (1 min), and extension at 72 C (2 min), and an additional extension step of 72 C for 7 min. The amplified products were analyzed by 3% agarose gel electrophoresis and ethidium bromide staining. The expected sizes of the products were 130 bp for exon 2 of VDR and 150 bp for the neomycin resistance gene.

Determination of P450arom activity

Activities of P450arom in ovaries were determined from the liberation of $[^3H]H_2O$ from [1β-^{3}H]androstenedione essentially according to previously reported methods (11, 12). The ovaries were homogenized with 10 times the volume of 10 mM potassium phosphate buffer (pH 7.4). The reaction was carried out by incubating a 200-μl reaction mixture containing potassium phosphate buffer (pH 7.4), [1β-^{3}H]androstenedione (200 nM; 0.988 Ci), NADPH (10 mM), and 20 μl of the homogenate (10–20 μg protein) at 37 C for 5–30 min and was terminated by adding 100 μl 25% (wt/vol) trichloroacetic acid. To remove unreacted [1β-^{3}H]androstenedione, the reaction mixture was treated with 100 μl dextran-charcoal, then centrifuged at 1200 × *g* for 5 min to obtain the supernatant. To further remove [1β-^{3}H]androstenedione, a 300-μl aliquot of the supernatant was diluted with 700 μl water and extracted with 2.5 ml chloroform. The radioactivity of the aqueous layer containing $[^3H]H_2O$ was measured in a liquid scintillation counter. A reaction mixture without the homogenate was used as a blank. From linear plots of the amounts of the product against reaction times, P450arom activities were determined in terms of picomoles of $[^3H]H_2O$ liberated per min/mg protein. Protein contents were determined using a bicinchoninic acid kit (Pierce Chemical Co., Rockford, IL).

The method for determination of P450arom activities in the testis and epididymis was the same as that employed for the ovary samples, except for cofactors and incubation time, because of the lower activity of the aromatase. The activities of P450arom in microsomal fractions prepared from the testis or the epididymis of male mice (10 weeks old) were determined as previously described (13). A 200-μl reaction mixture containing 10 mM potassium phosphate buffer (pH 7.4), $MgCl_2$ (85 mM), $NADP^+$ (10 mM), NADPH (10 mM), glucose-6-phosphate (100 mM), [1β-^{3}H]androstenedione (200 nM; 0.988 Ci), glucose-6-phosphate dehydrogenase (2 U), and 20 μl of the microsomal fractions as the enzyme source was incubated at 37 C for 1 h. A sample for determination of radioactivity was prepared in the manner described above. P450arom activity was defined in terms of picomoles of $[^3H]H_2O$ liberated per h/mg protein.

RT-PCR analysis for CYP19 gene expression and estrogen receptor α (ERα) and ERβ gene expression

Total RNA was extracted from the ovary and the testis by the acid-guanidine phenol-chloroform method (14). A RT-PCR analysis was carried out using 2 μg total RNA from the ovary and 5 μg total RNA from the testis, which was reverse transcribed using a random primer and Moloney murine leukemia virus reverse transcriptase in 25 μl, according to the manufacturer's protocol. An aliquot of the RT reaction was then used as the template for a subsequent PCR.

The complementary DNA (cDNA) for the mouse CYP19 gene was analyzed by PCR using a 50-μl reaction mixture containing cDNA template (2 μl from the ovary sample, 4 μl from the testis sample), specific primers of 5′-TGA GAG ACG TGG AGA CCT GA-3′ and 5′-CAC CTG GAA TCG TCT CAA AA-3′ (0.4 μM each), *Taq* polymerase (1 U), 5 μl 10 × PCR buffer, $MgCl_2$ (1.75 mM), and a deoxy-NTP mixture (0.2 mM). The reaction procedure for the amplification was as follows: an initial denaturation step at 95 C for 5 min; 35 cycles of 95 C (1 min), 56 C (2 min), and 72 C (2 min); and an extension step at 72 C for 10 min. The products were analyzed by 2% agarose gel electrophoresis and ethidium bromide staining. The expected size of the products was 526 bp. Direct sequencing of the 526-bp PCR product revealed a corresponding sequence in P450arom messenger RNA (mRNA). The image of the UV-illuminated gels was stored in a digital form and analyzed by a computerized image analyzing system (ATTO densitograph, ATTO Corp., Tokyo, Japan).

The cDNA for ERα and ERβ genes were analyzed by previously described methods (15, 16).

Glyceraldehyde-3-phosphate dehydrogenase (GAPDH) mRNA was coamplified to serve as an internal control. Each band was normalized to the value of GAPDH.

Competitive PCR analysis for quantitative CYP19 gene expression

The cDNA for mouse CYP19 gene after the calcium supplementation was analyzed by competitive PCR. The competitive sequence was constructed by PCR using PCR MIMICS as a template according to the manufacturer's protocol. The competitive template used was $4, 4 \times 10^{-1}$, 4×10^{-2}, 4×10^{-3}, 4×10^{-4} fM in each 50-μl reaction mixture. The expected size of the products was 350 bp.

Serum chemistries

LH levels and FSH levels were measured using an enzyme-linked immunosorbent assay for rat LH and FSH (Amersham Pharmacia Biotech, Aylesbury, UK). Estradiol levels were measured by RIA (Diagnostic Products, Los Angels, CA) at Mistubishi BCL (Tokyo, Japan). Calcium levels were measured using the *o*-cresol phthalein complexion method (Wako, Osaka, Japan). Phosphorous levels were measured using the *p*-methylaminophenol method (Wako).

Sperm function

Sperm counts and motility were determined. Sperm were collected from the epididymides of 11-week-old heterozygous and VDR null mutant mice. Sperm suspensions were prepared by mincing the excised cauda epididymides in 0.5 ml capacitation medium (17, 18). After allowing 15 min for sperm dispersion, particulate tissue was removed, and aliquots of the epididymal suspension were diluted 1:5 in the medium. Sperm counts and the estimated percentage of motile sperm were determined visually by phase microscopy.

Histological analysis

Testes were removed from mice, preincubated with OCT compound (Miles, Elkhart, IL), and then frozen with liquid nitrogen. Five-micron sections, cut with a cryostat, were collected on poly-L-lysine-coated slide glasses. The sections were stained with methyl green.

Estrogen supplementation

17β-Estradiol was given to VDR null mutant male mice at 5–10 weeks of age (10 ng/head·day) (19) by microosmotic pump (Alzet, Palo Alto, CA). After 5 weeks of treatment with 17β-estradiol, mice were killed, and the histology of the testes, sperm function, aromatase activity in the testes, the expression level of the CTP19 gene in the testes, and serum levels of calcium, LH, and FSH were analyzed. 17β-Estradiol was given to 7-week-old VDR null mutant female mice (100 ng/head·day) (19) by ip injection for 7 days. After treatment with 17β-estradiol, mice were killed, and aromatase activity in the ovaries was measured.

Statistical analysis

Values are given as the mean ± SEM. Statistical analysis was performed using unpaired Student's *t* test and ANOVA, followed by Fisher's protected least significant difference. $P < 0.05$ was considered significant.

Results

Low P450arom activity and CYP19 gene expression in gonads of the VDR null mutant mice

The activities of P450arom in the ovaries, testes, and epididymides were measured, and the results obtained are

shown in Fig. 1A. In the ovaries of the wild-type ($VDR^{+/+}$) mice, the enzyme activities at 4 and 7 weeks of age were 0.102 ± 0.018 (mean ± SEM; n = 4) and 0.357 ± 0.048 (n = 4) pmol $[^3H]H_2O$ liberated/min·mg protein, respectively. In the 7-week-old heterozygous ($VDR^{+/-}$) mice, the activity was 0.295 ± 0.035 (n = 4). No significant difference was found between the $VDR^{+/+}$ and $VDR^{+/-}$ mice in P450arom activity. Samples from the $VDR^{+/+}$ and $VDR^{+/-}$ female mice at 7 weeks of age were obtained at the time of estrus, as evidenced by labial swelling and reddening of vaginal membranes. The VDR null mutant ($VDR^{-/-}$) female mice never showed such a genital appearance. P450arom activity in the 7-week-old $VDR^{-/-}$ mice was 0.087 ± 0.011 (n = 4). This value was 24.4% of that in the 7-week-old $VDR^{+/+}$ mice and was similar to that in the 4-week-old $VDR^{+/+}$ mice (just after weaning).

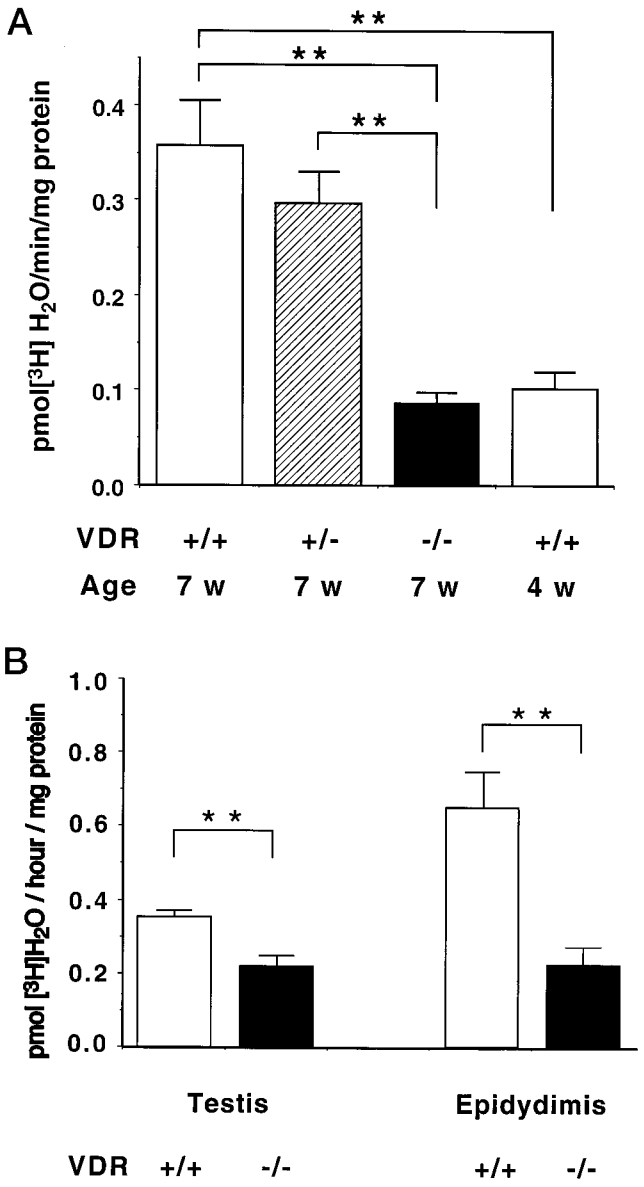

FIG. 1. Activities of P450arom in ovaries (A). Values are the mean ± SEM. The *black bar* presents the activity of enzyme in $VDR^{-/-}$ mice at 7 weeks of age. The *white bars* present those of $VDR^{+/+}$ mice at 4 and 7 weeks of age. The *hatched bar* presents that of $VDR^{+/-}$ mice at 7 weeks of age. Activities of P450arom were measured in $VDR^{+/+}$ and $VDR^{+/-}$ female mice at 7 weeks of age that were in estrous, as evidenced by labial swelling and reddening of vaginal membranes. Activities of P450arom in testes and epididymis of 10-week-old mice (B). The P450arom activity was defined in terms of picomoles of $[^3H]H_2O$ liberated per h/mg protein because of lower levels of the activities per mg protein. Values in testes and epididymis are approximately 1/60th of those in ovaries. **, $P < 0.01$ compared with wild-type mice. n = 4–5.

As shown in Fig. 1B, P450arom activity in the testes of 10-week-old $VDR^{+/+}$ mice was 0.354 ± 0.020 pmol $[^3H]H_2O$ liberated/h·mg protein (mean ± SEM; n = 4), which is approximately 1/60th the value in the ovaries of 7-week-old $VDR^{+/+}$ female mice. P450arom activity in the testes of 10-week-old $VDR^{-/-}$ mice was 0.207 ± 0.028 (n = 5) pmol $[^3H]H_2O$ liberated/h·mg protein. This level was 58.5% of that in 10-week-old $VDR^{+/+}$ mice ($P < 0.005$). In the epididymis, the level of P450arom activity in 10-week-old $VDR^{-/-}$ mice was 0.225 ± 0.049, which was 34.6% of that in $VDR^{+/+}$ mice (0.650 ± 0.118; n = 4; $P < 0.01$).

To evaluate the level of CYP19 gene expression, we applied a RT-PCR procedure. The results presented in Fig. 2 indicated that the ovary and testis of $VDR^{-/-}$ mice expressed the mRNA of the CYP19 gene, but the expression levels of the CYP19 gene were markedly decreased. Data from scans of the PCR gels are provided in Table 1. The expression levels of CYP19 gene in the ovary and testis of heterozygous ($VDR^{+/-}$) mice were similar to those in $VDR^{+/+}$ mice (data not shown). The PCR reactions without RT had no products. The results of competitive PCR were consistent with those of this RT-PCR.

Abnormalities in gonads in the male VDR null mutant mice

Sperm functions. After incubation in capacitation medium for 15 min, 50–60% of the sperm from the cauda epididymides of male $VDR^{+/-}$ mice were motile, whereas the percentage of sperm motile in the $VDR^{-/-}$ males declined from 15% to less than 1% at 10 weeks of age. As shown in Table 2, the

FIG. 2. *Left*, RT-PCR amplification of mRNA of CYP19 gene in the ovary (35 cycles). Lane 1, PCR amplification without RT. Lanes 2 and 3, RT-PCR amplification of mRNA of CYP19 gene in the ovary of $VDR^{-/-}$ at 7 weeks of age; lanes 4 and 5, RT-PCR amplification of mRNA of CYP19 gene in the ovary of $VDR^{+/+}$ at 7 weeks of age. *Right*, RT-PCR amplification of mRNA of CYP19 gene in the testes (35 cycles). Lanes 1 and 2, RT-PCR amplification of mRNA of CYP19 gene in the testes of $VDR^{-/-}$ at 10 weeks of age; lanes 3 and 4, RT-PCR amplification of mRNA of CYP19 gene in the testes of $VDR^{+/+}$ at 10 weeks of age; lane 5, PCR amplification without RT. Each lane of the same phenotype represents a different animal. Figures show data representative of three independent experiments. Reduced CYP19 gene mRNA expressions in the ovary and the testis of $VDR^{-/-}$ mice were observed in both sexes. The scanned data are shown in Table 1.

TABLE 1. The scanned data of RT-PCR amplification of mRNA of CYP19 gene in the ovary (7 weeks of age) and the testes (10 weeks of age)

Ovary		Testis	
$VDR^{-/-}$	$VDR^{+/+}$	$VDR^{-/-}$	$VDR^{+/+}$
0.019 ± 0.005 (10)	0.462 ± 0.044 (10)	0.062 ± 0.011 (10)	0.537 ± 0.026 (10)
$P < 0.001$		$P < 0.001$	

The scanned data are expressed as the ratio of CYP19/GAPDH. Values are given as the mean ± SEM. The numbers in *parentheses* show the number of animals analyzed.

TABLE 2. Sperm function

Sperm count ($\times 10^6$/ml)		Sperm motility (%)	
$VDR^{+/-}$	$VDR^{-/-}$	$VDR^{+/-}$	$VDR^{-/-}$
50.8 ± 5.5 (4)	26.3 ± 7.3 (3)	53.7 ± 2.7 (4)	6.0 ± 4.5 (3)
$P < 0.05$		$P < 0.01$	

Values are given as the mean ± SEM. The numbers in *parentheses* show the number of animals analyzed. *P* values are results of *t* tests for $VDR^{+/-}$ *vs.* $VDR^{-/-}$.

sperm counts in $VDR^{-/-}$ mice were half those in $VDR^{+/-}$ mice. These results revealed that the number of functional sperm was markedly decreased in $VDR^{-/-}$ mice compared with $VDR^{+/-}$ mice. The motility and sperm count in $VDR^{+/-}$ mice were similar to those in wild-type mice (18).

Testicular weight. Testicular weights were evaluated as the ratio of testis weight (milligrams) to body weight (grams). A transient increase in testicular weight in $VDR^{-/-}$ males was observed at 10 weeks of age ($P < 0.01$ compared with $VDR^{+/-}$ mice), although weight had decreased to the normal level by 15 weeks, as reported in ERα gene knockout mice (Fig. 3).

Histology of the testes. Although the appearance of the testes was normal anatomically, histological change was observed in the testes of $VDR^{-/-}$ mice. As shown in Fig. 4B, the testes of 10-week-old $VDR^{-/-}$ mice showed dilated lumen of seminiferous tubules, a thinner layer of epithelial cells, and decreased spermatogenesis. The testes of 15-week-old $VDR^{-/-}$ mice revealed rare spermatogenesis. A more widely dilated lumen of seminiferous tubules and atrophy of the seminiferous epithelium cells were observed (Fig. 4C).

Decreased serum levels of estradiol and elevated serum levels of LH and FSH

The serum levels of estradiol in the VDR null mutant mice are shown in Table 3. The circulating estradiol level in VDR null mutant female mice was significantly lower than that in heterozygous mice. Serum levels of LH and FSH in VDR null mutant mice are shown in Table 4. The LH and FSH levels in 3-week-old VDR null mutant mice were the same as those in $VDR^{+/+}$ mice. The LH level was elevated 5- to 10-fold in both female and male $VDR^{-/-}$ mice compared with that in $VDR^{+/+}$ mice at 8 weeks of age. The FSH level in $VDR^{-/-}$ mice was twice that in $VDR^{+/+}$ mice at 8 weeks of age. These elevated levels of LH and FSH in $VDR^{-/-}$ mice were sustained to 12 weeks of age. The estradiol, LH, and FSH levels were measured in wild-type female mice that were in estrous, as evidenced by labial swelling and reddening of vaginal membranes.

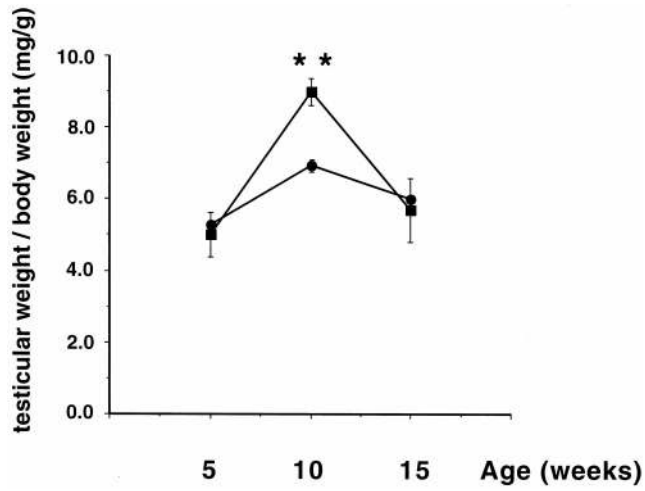

FIG. 3. Testicular weight between 5 and 15 weeks of age. Values are defined as the ratio of testis weight (milligrams)/body weight (grams) so as to eliminate body weight differences between $VDR^{+/-}$ mice and $VDR^{-/-}$ mice (mean ± SEM). *Closed circles* represent $VDR^{+/-}$ mice, and *closed squares* represent $VDR^{-/-}$ mice. The ratio of $VDR^{-/-}$ mice increased at 10 weeks of age. **, $P < 0.01$ *vs.* $VDR^{+/-}$ mice (n = 4–8).

Effect of estrogen supplementation

After estrogen supplementation of VDR null mutant male mice, the histology of the testes revealed no apparent abnormality of the lumen of the seminiferous tubules or epithelial cells at 10 weeks of age, as shown in Fig. 4D. The sperm count and motility in the estrogen-treated mice (n = 3) were increased to the same level in the heterozygous mice [count, 47.7 ± 5.0 × 10^6/ml *vs.* 26.3 ± 7.3 × 10^6/ml in $VDR^{-/-}$ without treatment ($P < 0.05$); motility: 47.0 ± 3.6% *vs.* 6.0 ± 4.6% in $VDR^{-/-}$ without treatment ($P = 0.0001$)]. The P450arom activity in the testes of $VDR^{-/-}$ mice with estrogen treatment was increased (0.328 ± 0.018 pmol $[^3H]H_2O$ liberated/h·mg protein *vs.* 0.207 ± 0.028 in the $VDR^{-/-}$ without treatment; n = 3; $P = 0.03$). The expression level of the CYP19 gene in the testis with estrogen supplementation was analyzed by competitive PCR. The level in $VDR^{-/-}$ was 0.6 ± 0.2 attomoles (attmol; 10^{-18} M). After estrogen treatment, the expression level was significantly increased to 16.7 ± 3.3 attomol ($P < 0.0001$). This level was similar to the level in VDR+/+ (23.3 ± 8.8 attomol; $P = 0.613$). The serum LH level was decreased to 4.13 ± 0.20 ng/ml (n = 3), and the serum FSH level was decreased to 208.7 ± 10.5 ng/ml (n = 3) after the supplementation ($P = 0.0003$ and <0.0001 respectively, compared with $VDR^{-/-}$ male mice at 8 weeks of age). The serum calcium level was not increased (6.4 ± 0.1 *vs.* 8.30 ± 0.26 mg/dl in the $VDR^{+/+}$ mice; $P = 0.0008$). As

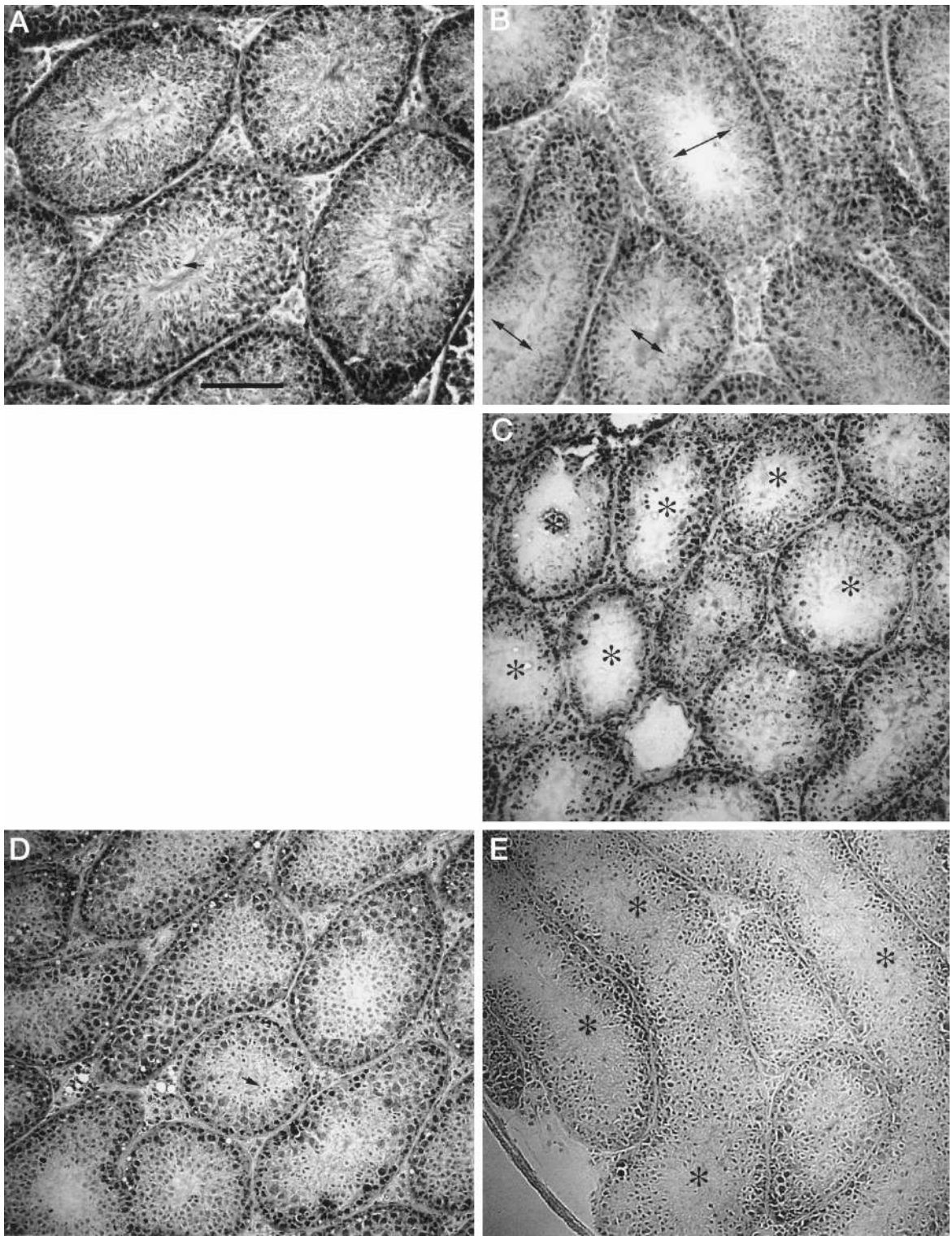

FIG. 4. Histology of testes from $VDR^{+/-}$ mice and $VDR^{-/-}$ mice in methyl green stain. A, The testis of a 10-week-old $VDR^{+/-}$ mouse. The seminiferous tubules were at different stages of spermatogenesis, and the diameter of the lumen and the thickness of the seminiferous epithelium vary with the stage of spermatogenesis (*arrow*); B, the testis of a 10-week-old $VDR^{-/-}$ mouse. The lumen of the seminiferous tubules was often dilated (*arrows*). The thickness of the seminiferous epithelium is less than in 10-week-old control mice. C, The testis of a 15-week-old $VDR^{-/-}$ mouse. The lumen was more widely dilated (*asterisks*), the seminiferous epithelium is atrophic in many tubules, and spermatogenesis is rare. D, The testis of a 10-week-old $VDR^{-/-}$ mouse with estrogen treatment revealed no change. The seminiferous tubules were at different stages of spermatogenesis (*arrow*), and the diameter of the lumen and the thickness of the seminiferous epithelium vary with the stage of spermatogenesis. E, The testis of a 10-week-old $VDR^{-/-}$ mouse with calcium supplementation revealed dilated lumen in some seminiferous tubules (*asterisks*). *Bar,* 100 μm.

in the male mice, the P450arom activity in the ovary of $VDR^{-/-}$ mice (n = 3) with estrogen treatment was increased (0.293 ± 0.028 pmol $[^3H]H_2O$ liberated/min·mg protein *vs.* 0.087 ± 0.011 in the $VDR^{-/-}$ without treatment; $P < 0.0001$).

The expression levels of ERα and ERβ in the ovary and testis of the VDR null mutant mice were the same as those in the wild-type mice (Fig. 5). In the ovary, the ratios of the expression level of ERα/GAPDH in $VDR^{-/-}$ and $VDR^{+/+}$ were 0.877 ± 0.167 and 0.998 ± 0.078, respectively, and the ratios of the expression level of ERβ/GAPDH in $VDR^{-/-}$ and $VDR^{+/+}$ were 7.190 ± 0.622 and 8.647 ± 0.891, respectively. In the testis, the ratios of the expression level of ERα/GAPDH in $VDR^{-/-}$ and $VDR^{+/+}$ were 0.613 ± 0.029 and 0.642 ± 0.057, respectively, and the ratios of the expression level of ERβ/GAPDH were 0.968 ± 0.109 and 1.027 ± 0.084, respectively. The scanned data revealed that there was no significant difference between $VDR^{-/-}$ and $VDR^{+/+}$ mice in either ER expression.

Effect of calcium supplementation

The serum calcium level in the VDR null mutant mice given a normal diet (MF) was 5.36 ± 0.25 mg/dl (mean ± SEM; n = 9) at the age of 7 weeks. The serum calcium level in $VDR^{+/+}$ mice was 8.30 ± 0.26 mg/dl (n = 10) at this age. To correct the hypocalcemia, the VDR null mutant mice (n = 10) were fed a high calcium diet from the time of weaning (3 week of age). Serum calcium increased to 8.65 ± 0.25 mg/dl (n = 8). The serum calcium level in VDR null mutant mice was completely normalized after calcium supplementation. P450arom activity in the ovary at the 7 weeks of age was 0.223 ± 0.015 pmol $[^3H]H_2O$/min·mg protein after calcium supplementation. P450arom activity was increased to 60% of that in wild-type mice ($P = 0.005$) and 76% of that in heterozygous mice ($P = 0.091$). P450arom activity in the testis at 10 weeks of age was 0.272 ± 0.013 pmol $[^3H]H_2O$/h·mg protein after calcium supplementation. P450arom activity was increased to 77% of that in wild-type mice ($P = 0.024$). The competitive PCR analysis of CYP19 is shown in Fig. 6 and Table 5. These results indicated that the expression of the CYP19 gene was increased by calcium supplementation in both ovary and testis. However, as with aromatase activity, the expression level of the aromatase gene was not completely recovered after normalization of serum calcium, being one fifth that of the wild-type value in the ovary ($P = 0.004$) and one fourth that of the wild-type value in the testis ($P = 0.02$). As shown in Table 3, the circulating estradiol level did not increase after calcium supplementation. In the female the estradiol level was 5.6 ± 2.6 pg/ml (n = 4; $P = 0.03$ compared with that in $VDR^{+/-}$ female mice at 8 weeks of age). The serum levels of LH and FSH were not corrected and remained high despite the fact that the serum calcium level was normal after calcium supplementation. In the female, the LH level was 5.9 ± 0.2 ng/ml, and the FSH level was 385 ± 32 ng/ml (n = 3; $P < 0.0001$ and 0.001, respectively, compared with that in $VDR^{+/+}$ female mice at 8 weeks of age). In male mice, the LH level was 8.1 ± 0.3 ng/ml (n = 3; $P < 0.0001$ compared with $VDR^{+/+}$ male mice at 8 weeks of age), and the FSH level was 310 ± 16 ng/ml (n = 3; $P < 0.0001$ compared with $VDR^{+/+}$ male mice at 8 weeks of age). In male VDR null mutant mice given calcium supplements, dilated lumens were observed in certain seminiferous tubules (Fig. 4E). The sperm

TABLE 3. Serum estradiol values

	Male (10 weeks)	Female (8 weeks)
$VDR^{+/-}$	7.3 ± 1.5 (5)	19.4 ± 1.8 (5)
$VDR^{-/-}$	4.5 ± 2.4 (4)	3.3 ± 1.3[a] (5)
$VDR^{-/-}$ with Ca supplement	6.7 ± 2.7 (4)	5.6 ± 2.6[a] (4)

Values are given as the mean ± SEM (picograms per ml). The numbers in *parentheses* show the number of animals analyzed.
[a] $P < 0.01$ compared with $VDR^{+/-}$ female mice at 8 weeks of age.

TABLE 4. Serum LH and FSH values

	3 weeks	8 weeks	12 weeks
$VDR^{+/+}$			
Female			
LH	0.7 ± 0.1 (4)	1.2 ± 0.3 (4)	ND
FSH	165.0 ± 18.0 (4)	262.8 ± 6.1 (4)	ND
Male			
LH	ND	0.97 ± 0.04 (4)	ND
FSH	ND	208.5 ± 12.8 (4)	ND
$VDR^{-/-}$			
Female			
LH	0.98 ± 0.04 (3)	5.8 ± 0.4[a] (4)	8.4 ± 1.0 (4)
FSH	204.0 ± 24.0 (3)	409.8 ± 43.6[a] (4)	473.0 ± 25.0 (4)
Male			
LH	ND	8.5 ± 0.8[a] (4)	7.1 ± 0.5 (3)
FSH	ND	426.3 ± 23.5[a] (4)	445.5 ± 5.5 (3)
$VDR^{-/-}$ male with estrogen supplementation (10 weeks)			
	LH 4.1 ± 0.2[a,b] (3)	FSH 208.7 ± 10.5[b] (3)	
$VDR^{-/-}$ with calcium supplementation (8 weeks)			
Female	LH 5.9 ± 0.2[a] (3)	FSH 385.0 ± 32.0[a] (3)	
Male	LH 8.1 ± 0.3[a] (3)	FSH 310.0 ± 16.0[a] (3)	

Values are given as the mean ± SEM (nanograms per ml). The numbers in *parentheses* show the number of animals analyzed. ND, Not determined.
[a] $P < 0.01$ compared with $VDR^{+/+}$ mice at 8 weeks of age.
[b] $P < 0.001$ compared with $VDR^{-/-}$ mice at 8 weeks of age. LH was measured in wild-type female mice at 8 weeks of age that were in estrous, as evidenced by labial swelling and reddening of vaginal membranes.

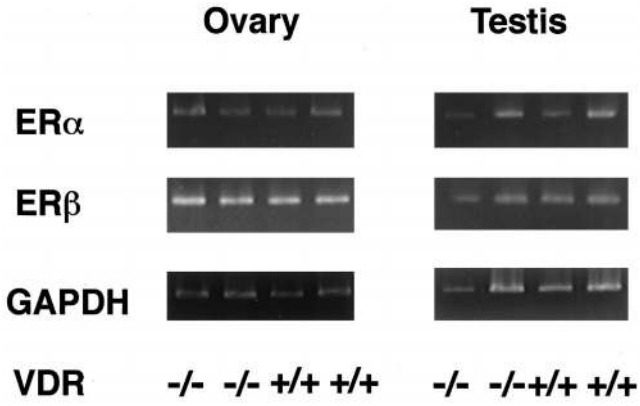

FIG. 5. *Left*, RT-PCR amplification of mRNA of the ERα and ERβ gene in the ovary. Lanes 1 and 2, RT-PCR amplification of mRNA of the ERα and ERβ genes in the ovary of $VDR^{-/-}$ at 7 weeks of age; lanes 3 and 4, RT-PCR amplification of mRNA of the ERα and ERβ genes in the ovary of $VDR^{+/+}$ at 7 weeks of age. *Right*, RT-PCR amplification of mRNA of the ERα and ERβ genes in the testes. Lanes 1 and 2, RT-PCR amplification of mRNA of the ERα and ERβ genes in the testes of $VDR^{-/-}$ at 10 weeks of age; lanes 3 and 4, RT-PCR amplification of mRNA of the ERα and ERβ genes in the testes of $VDR^{+/+}$ at 10 weeks of age. Each lane of the same phenotype represents a different animal. Figures show data representative of three independent experiments. The expression of ERα and ERβ in the ovary and the testis in the VDR null mutant mice was the same as that in wild-type mice. The scanned data are shown in Table 3.

count was increased to $44.0 \pm 5.3 \times 10^6$/ml, but was not significantly different compared with that in $VDR^{-/-}$ animals without treatment ($P = 0.09$). Sperm motility was significantly increased to 39.3% compared with that in $VDR^{-/-}$ mice without treatment ($P = 0.0015$).

Discussion

Previous studies suggested that vitamin D has some role in reproductive functions. The VDR is expressed in the ovary and testis (6), suggesting that vitamin D has a role in these organs. Vitamin D deficiency caused gonadal insufficiency in rats. The overall fertility of the female vitamin D-deficient rats was reduced to 75%, and the litter size was reduced to 30% of the values in vitamin D-replete females (19). The presence of sperm in the vaginal tract of females mated by vitamin D-deficient males was reduced to 45% compared with that in matings by vitamin D-replete males (20).

In female VDR null mutant mice, uterine hypoplasia with impaired folliculogenesis was observed, and estrogen supplementation increased uterine weight (7). These results indicated that estrogen deficiency caused impaired folliculogenesis and uterine hypoplasia in female VDR null mutant mice. In male VDR null mutant mice in this study, a transient increase in testicular weight was observed, and decreased sperm counts and motility with histological abnormality in the testis were found. These findings in VDR null mutant male mice were similar to those in ERα knockout mice (18, 21, 22). In the male gonads of ERα knockout mice, the fluid reabsorption in efferent ductules of the testis was abnormal (22). In our study of VDR null mutant male mice, estrogen deficiency appeared to cause gonadal insufficiencies by a mechanism similar to that observed in ERα knockout mice. In addition, aromatase gene-deficient mice (ArKO) showed gonadal insufficiencies, such as underdeveloped uteri and ovaries (23) and impaired spermatogenesis (24). The phenotypes of gonads of ERα and ArKO paralleled those of the VDR null mutant male mice.

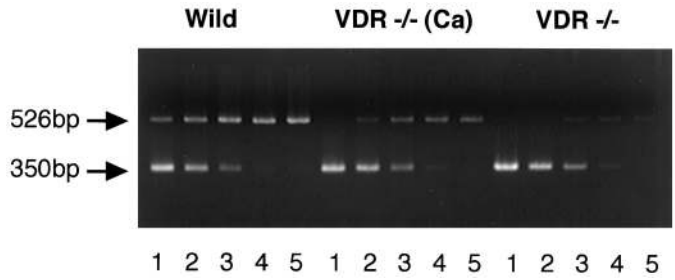

FIG. 6. The effect of calcium supplementation. The competitive RT-PCR amplification of mRNA of the CYP19 gene in ovary at 7 weeks of age in wild ($VDR^{+/+}$) and $VDR^{-/-}$ mice with calcium supplementation and $VDR^{-/-}$ mice without treatment. The CYP19 gene product was 526 bp, and competitor product was 350 bp. The competitive template used was 4, 4×10^{-1}, 4×10^{-2}, 4×10^{-3}, and 4×10^{-4} fM from lane 1 to lane 5, respectively. The expression of the CYP19 gene in the ovary of $VDR^{-/-}$ mice given calcium supplements was increased. This photograph shows data representative of three independent experiments.

TABLE 5. The effect of Ca supplementation on the level of CYP19 gene expression

	$VDR^{+/+}$	$VDR^{-/-}$ with Ca supplementation	$VDR^{-/-}$
Ovary	118 ± 56 (4)	25 ± 13[a] (4)	1.9 ± 1.5 (4)
Testis	23.3 ± 8.8 (3)	6.3 ± 1.9[b] (3)	0.6 ± 0.2 (3)

The expression levels of CYP19 gene were analyzed by competitive PCR. Values are given as the mean ± SEM (attomoles; 10^{-18} M). The numbers in *parentheses* show the number of animals analyzed. The data were analyzed by ANOVA after conversion to a log scale.
[a] $P = 0.004$ *vs.* $VDR^{+/+}$ mice; $P = 0.0001$ *vs.* $VDR^{-/-}$ mice.
[b] $P = 0.02$ *vs.* $VDR^{+/+}$ mice; $P = 0.0006$ *vs.* $VDR^{-/-}$ mice.

No histological abnormality was observed in the testes of male VDR null mutant mice supplemented with estrogen. The estrogen supplementation protected the testis of VDR null mutant mice from histological changes. These results strongly suggested that estrogen deficiency induced by VDR ablation is the cause of the abnormal spermatogenesis in VDR null mutant mice.

Decreases in the activity of P450arom and suppression of CYP19 gene expression in both female and male gonads of the VDR null mutant mice were demonstrated. The CYP19 gene encodes P450arom, the key enzyme for estrogen biosynthesis, which dominantly influences the estrogen level. Furthermore, the expressions of ERα and ERβ genes were normal in gonads in VDR null mutant mice. These results indicated that the estrogen-deficient state in VDR null mutant mice caused by decreased P450arom activity depended on suppressed CYP19 gene expression.

It was reported that normalization of the serum calcium level restored fertility in vitamin D-deficient female and male rats (25, 26) and also prevented some phenotypic abnormalities in the VDR null mutant mice (9). To clarify the influences of severe hypocalcemia, calcium supplementation was performed in the VDR null mutant mice. A high calcium diet increased the serum calcium level to near that in wild-type mice. The normalization of the serum calcium level increased

aromatase activity in the ovary to 60% of that in the wild-type animals. Furthermore, the expression level of the CYP19 gene was increased to 10-fold that in VDR null mutant mice without calcium supplementation. The high levels of LH and FSH after normalization of serum calcium meant that the endocrinological state remained abnormal.

Despite the abnormal endocrinological state, some VDR null mutant mice with a normal serum calcium level were fertile. This may explain why other VDR-ablated mice (27) did not show infertility, although the details of the gonadal functions were not reported. The serum calcium levels of these mice were much higher than those of our VDR null mutant mice [1.00–1.09 mM (82% of wild-type mice) *vs.* 5.36 ± 0.25 mg/dl (65% of wild-type mice)]. In human cases of vitamin D-dependent rickets type II, no gonadal insufficiencies were detected (28, 29). Calcium had been administered to these patients from an early phase. Normalization of the serum calcium level might therefore restore the infertility. It is possible that hypogonadism was generated by nonspecific disruption of the aromatase gene enhancer region. However, it is difficult to consider this possibility. Li model VDR-ablated mice (27) and our VDR null mutant mice revealed similar phenotypes, such as growth retardation, impairment of bone formation, and alopecia, though the phenotypes of the Li model were much milder. In addition, normalization of mineral ion homeostasis prevented the phenotypes, except for alopecia (9). The higher level of serum calcium might cause the milder phenotypes and fertility of the Li model.

It was recently reported that the P450arom activity of human choriocarcinoma cell lines was stimulated by 1,25-$(OH)_2D_3$ and that the VDR response element was identified in the CYP19 gene (30). This would suggest that vitamin D regulates the CYP19 gene directly. Using VDR null mutant mice, not vitamin D-deficient mice, we demonstrated that vitamin D acted to regulate estrogen biosynthesis: this regulation could not be explained by the calcitropic activities alone. These results indicated that vitamin D plays a role in estrogen biosynthesis partially by maintaining extracellular calcium homeostasis. However, direct regulation of the expression of the aromatase gene was also considered.

Acknowledgment

We are grateful to Ms. L. Abe for secretarial assistance.

References

1. **Walters MR** 1992 Newly identified actions of the vitamin D endocrine system. Endocr Rev 13:719–764
2. **Bouillon R, Okamura WH, Norman AW** 1995 Structure-function relationships in the vitamin D endocrine system. Endocr Rev 16:200–257
3. **Studzinski GP, McLane JA, Uskokovic MR** 1993 Signaling pathways for vitamin D-induced differentiation: implications for therapy of proliferative and neoplastic diseases. CRC Crit Rev Eukaryotic Gene Expression 3:279–312
4. **Darwish H, DeLuca HF** 1993 Vitamin D-regulated gene expression. CRC Crit Rev Eukaryotic Gene Expression 3:89–116
5. **Mangelsdorf DJ, Evans RM** 1995 The RXR heterodimers and orphan receptors. Cell 83:841–850
6. **Stumpf WE** 1995 Vitamin D sites and mechanisms of action: a histochemical perspective. Reflections on the utility of autoradiography and cytopharmacology for drug targeting. Histochem Cell Biol 104:417–427
7. **Yoshizawa T, Handa Y, Uematsu Y, Takeda S, Sekine K, Yoshihara Y, Kawakami T, Arioka K, Soto H, Uchiyama Y, Masushige S, Fukamizu A, Matsumoto T, Kato S** 1997 Mice lacking the vitamin D receptor exhibit impaired bone formation, uterine hypoplasia and growth retardation after weaning. Nat Genet 16:391–396
8. **Nelson DR, Kamataki T, Waxman DJ, Guengerich FP, Estabrook RW, Feyereisen R, Gonzalez FJ, Coon MJ, Gunsalus IC, Gotoh O, Okuda K, Nebert DW** 1993 The P450 superfamily: update on new sequences, gene mapping, accession numbers, early trivial names of enzymes, and nomenclature. DNA Cell Biol 12:1–51
9. **Li YC, Amling M, Pirro AE, Priemel M, Meuse J, Baron R, Delling G, Demay MB** 1998 Normalization of mineral ion homeostasis by dietary means prevents hyperparathyroidism, rickets, and osteomalacia, but not alopecia in vitamin D receptor-ablated mice. Endocrinology 139:4391–4396
10. **Gendron-Maguire M, Gridley T** 1993 Transgenic animals: pronuclear injection. In: Wassarman M, DePamphilis ML (eds) Methods in Enzymology. Guide to Techniques in Mouse Development. Academic Press, San Diego, vol 225:794–799
11. **Thompson Jr EA, Siiteri PK** 1974 Utilization of oxygen and reduced nicotinamide adenine dinucleotide phosphate by human placental microsomes during aromatization of androstenedione. J Biol Chem 249:5364–5372
12. **Roselli CE, Ellnwood WE, Resko JA** 1984 Regulation of brain aromatase activity in rats. Endocrinology 114:192–200
13. **Janulis L, Hess RA, Bunick D, Nitta H, Janssen S, Asawa Y, Bahr JM** 1996 Mouse epididymal sperm contain active P450 aromatase which decreases as sperm traverse the epididymis. J Androl 17:111–116
14. **Chomczynski P, Sacchi N** 1987 Single-step method of RNA isolation by acid guanidium-thiocyanate-phenol-chloroform extraction. Anal Biochem 162: 156–159
15. **Shen ES, Meade EH, Pérez MC, Deecher DC, Negro-Vilar A, López FJ** 1998 Expression of functional estrogen receptors and galanin messenger ribonucleic acid in immortalized luteinizing hormone-releasing hormone neurons: estrogenic control of galanin gene expression. Endocrinology 139:939–948
16. **Rosenfeld CS, Ganjam VK, Taylor JA, Yuan X, Stiehr JR, Hardy MP, Lubahn DB** 1998 Transcription and translation of estrogen receptor-β in the male reproductive tract of estrogen receptor-α knock-out and wild-type mice. Endocrinology 139:2982–2987
17. **Saling PM, Storey BT, Wolf DP** 1978 Calcium-dependent binding of mouse epididymal spermatozoa to the zona pellucida. Dev Biol 65:515–525
18. **Eddy E.M, Washburn TF, Bunch DO, Goulding EH, Gladen BC, Lubahn DB, Korach KS** 1996 Targeted disruption of the estrogen receptor gene in male mice causes alteration of spermatogenesis and infertility. Endocrinology 137: 4796–4805
19. **Halloran BP, Deruca HF** 1980 Effect of vitamin D deficiency on fertility and reproductive capacity in the female rat. J Nutr 110:1573–1580
20. **Kwiecinski GG, Petrie GI and DeLuca HF** 1989 Vitamin D is necessary for reproductive functions of the male rat. J Nutr 119:741–744
21. **Martin L, Finn CA, Trnder G** 1973 Hypertrophy and hyperplasia in the mouse uterus after oestrogen treatment: an autoradiographic study. J Endocrinol 56:133–144
22. **Hess RA, Bunick D, Lee KH, Bahr J, Taylor JA, Korach KS, Lubahn DB** 1997 A role for oestrogens in the male reproductive system. Nature 390:509–512
23. **Fisher CR, Graves KH, Parlow AF, Simpson ER** 1998 Characterization of mice deficient in aromatase (ArKO) because of targeted disruption of the *cyp19* gene. Proc Natl Acad Sci USA 95:6965–6970
24. **Robertson KM, O'Donnell L, Jones MEE, Meachem SJ, Boon WC, Fisher CR, Graves KH, McLachlan RI, Simpson ER** 1999 Impairment of spermatogenesis in mice lacking a functional aromatase (*cyp19*) gene. Proc Natl Acad Sci USA 96:7986–7991
25. **Kwiecinski GG, Petrie GI, DeLuca HF** 1989 125-Dihydroxyvitamin D_3 restores fertility of vitamin D-deficient female rats. Am J Physiol 256:E483–E487
26. **Uhland AM, Kwiecinski GG, DeLuca HF** 1992 Normalization of serum calcium restores fertility in vitamin D-deficient male rats. J Nutr 122:1338–1344
27. **Li YC, Pirro AE, Amling M, Delling G, Baron R, Bronson R, Demay MB** 1997 Targeted ablation of the vitamin D receptor: An animal model of vitamin D-dependent rickets type II with alopecia. Proc Natl Acad Sci USA 94:9831–9835
28. **Malloy PJ, Hochberg Z, Tiosano D, Pike JW, Hughes MR, Feldman D** 1990 The molecular basis of hereditary 1,25-Dihydroxyvitamin D_3 resistant rickets in seven related families. J Clin Invest 86:2071–2079
29. **Hawa NS, Cockerill FJ, Vadher S, Hewison M, Rut AR, Pike JW, O'Riordan JL, Farrow SM** 1996 Identification of a novel mutation in hereditary vitamin D resistant rickets causing exon skipping. Clin Endocrinol 45:85–92
30. **Sun T, Zhao Y, Mangelsdorf DJ, Simpson ER** 1997 Characterization of regon upstream of exon I.1 of the human CYP19 (aromatase) gene that mediates regulation by retinoids in human choriocarcinoma cells. Endocrinology 139: 1684–1691